Abstract Submitted

for the Atlanta Meeting of the

American Physical Society

March 29 – April 1, 1976

Physics and Astronomy
Classification Scheme
Number __71.20__

Bulletin Subject Heading
in which paper should be placed

(SN)$_x$, Polysulfur Nitride

Calculated Optical Properties of (SN)$_x$. I. B. ORTENBURGER, W. E. RUDGE and P. M. GRANT, IBM Research Laboratory, San Jose, Calif.--The tensorial dielectric constant $\varepsilon_2(\omega)$ and the tensorial photoemission yield $D(E,\omega)$ have been calculated for (SN)$_x$ using a pseudo-potential interpolation scheme based on a first principles OPW band structure. $D(E,\omega)$ and $\varepsilon_2(\omega)$ were computed by the Gilat-Raubenheimer zonal integration method. Our results will be compared to experimental photoemission and optical[1] measurements on randomly oriented (SN)$_x$ films.

[1]A. A. Bright and A. F. Garito.

Submitted by

_____
 Signature of APS Member

Irene B. Ortenburger

IBM Research Laboratory

5600 Cottle Road

San Jose, Calif. 95193

bulletin

OF THE AMERICAN PHYSICAL SOCIETY

BE 4 Transport Properties of $Hg_{2.86}(AsF)_6$, R. Spal, T. Wei, C.K. Chiang, A.F. Garito and A.J. Heeger, N. Miro and A.G. MacDiarmid, University of Pennsylvania, Phila., Penna. --We report the temperature dependent dc electrical conductivity of the novel conductor $Hg_{2.86}(AsF_6)_2$ which consists of planes of interpenetrating one dimensional chains of Hg atoms. The measured conductivity parallel to the planes is 3.5×10^3 $(\Omega\text{-cm})^{-1}$ at room temperature and exhibits a negative temperature coefficient down to 4.2K with an anomaly near 220K. Anisotropy measurements using the Montgomery method will be reported in addition. The conductivity measurements will be compared with studies of a plasma edge in the visible optical reflectance and measurements using DSC.

BE 5 Anionic Linear Chain Iridium Carbonyl Halides. A. P. GINSBERG, J. W. KOEPKE, J. J. HAUSER, K. W. WEST, F. J. DI SALVO, C. R. SPRINKLE and R. L. COHEN, Bell Laboratories.--The compounds $K_{0.60}Ir(CO)_2Cl_2 \cdot 0.5H_2O$, $(TTF)_{0.61}Ir(CO)_2Cl_2$ (TTF = Tetrathiafulvalenium), $K_{0.57}Ir(CO)_2Br_2 \cdot 0.2CH_3COCH_3$ and $Cs_{0.60}Ir(CO)_2Br_2$ have been investigated by chemical analysis, infrared and ^{193}Ir Mössbauer spectroscopy, electrical conductivity and magnetic susceptibility measurements. Conducting linear chains of cis-$[Ir(CO)_2X_2]^{-0.60}$ (X = Cl, Br) units are shown to be present in these compounds. The apparently well defined compounds $K_{0.98}Ir(CO)_2Cl_2 \cdot 42 \cdot 0.2CH_3COCH_3$ and $Na_{0.93}Ir(CO)_2Cl_2 \cdot 32 \cdot 0.3CH_3COCH_3$, are reformulated as $K_{0.60}Ir(CO)_2Cl_2 \cdot 0.4KCl \cdot 0.2CH_3COCH_3$ and $Na_{0.61}Ir(CO)_2Cl_2 \cdot 0.32NaCl \cdot 0.3CH_3COCH_3$, in which the KCl and NaCl are present interstitially in the lattice of linear chains.

BE 6 EPR pair spectra in a dimeric chromium phosphinate.* P. D. KRASICKY, A. L. RITTER, J. C. SCOTT and R. H. SILSBEE, Cornell University-- The dimeric material, di-μ-diphenylphosphinatoacetylacetonatochromium $(III)^{(1)}$, consists of molecules in which the two chromium atoms, each of spin $S_{1,2} = 3/2$ are linked by phosphinate (-OPΦ_2O-) bridges, and is therefore the simplest member of the family of one-dimensional poly(chromium phosphinates).(2) The "endcapping" acetylacetonate ligands complete the closely octahedral environment of six oxygen atoms around each chromium. Within the molecule the chromium-chromium separation is 5Å, compared to ~10Å between molecules. The EPR pair spectrum at X band indicates an antiferromagnetic exchange, $J \simeq$ 4K, comparable to that in the polymers. At temperatures T≲4K the S=3 (total spin) multiplet is virtually unpopulated, and we have identified transitions within the S=1 and S=2 multiplets. The data are interpreted in terms of a spin Hamiltonian derived by coupling the single ion Hamiltonians with an exchange term.

*Supported by the National Science Foundation.
[1]C.E. Wilkes and R.A. Jacobson, Inorg. Chem.4,99(1965).
[2]J.C. Scott, T.S. Wei, A.F. Garito, A.J. Heeger, H.D. Gillman and P. Nannelli, Proc. Conf. on Magnetism and Magnetic Materials, Phila., 1975 (to be published)

BE 7 UPS Photoemission Properties of $(SN)_x$. P. MENGEL, W. D. GROBMAN, I. B. ORTENBURGER, P. M. GRANT and B. H. SCHECHTMAN, IBM Research Laboratory, San Jose, Calif.--We have performed UPS measurements on in situ deposited films of $(SN)_x$ as a function of incident photon energy in the range 7.6 - 40.8 eV. The results are in general agreement with previously reported XPS studies.[1] Relaxation effects lower the observed photoemissive yield at the Fermi level to zero. We analyze our data through comparison with theoretical energy distribution curves obtained from pseudopotential eigenvalues and eigenfunctions. We also report some initial results on the UPS spectrum of partially polymerized S_2N_2.
[1]P. Mengel, P. M. Grant, W. E. Rudge, B. H. Schechtman and D. W. Rice, Phys. Rev. Letters 35, 1803 (1975).

BE 8 XPS Core-Level Spectroscopy, Charge Transfer and Electrostatic Interactions in $(SN)_x$ and Other SN Allotropes. A.J. EPSTEIN, W.R. SALANECK, N.O. LIPARI and J.W-p LIN, Xerox Webster Research Center, Webster, N.Y. 14580.--The binding energies of S_{2p} and N_{1s} levels in $(SN)_x$ have been studied via x-ray photoemission spectroscopy and results compared with neutral S_8 and N_2 molecules respectively, as well as S_4N_4. The effective charge transfer from sulfur to nitrogen is $0.5|e|$ in $(SN)_x$ as compared to $0.6|e|$ in S_4N_4. Shake-up structure on the core level lines of $(SN)_x$ is assigned to excitation of conduction electron plasmons. Using the above XPS measured net charges, the electrostatic interactions in S_2N_2, S_4N_4 and $(SN)_x$ were calculated. Though the total electrostatic potential at any site due to all other atoms in a crystal is large and nearly identical for all three allotropes, the net electrostatic interaction between molecules (polymer chains) is small and nearly identical in all three cases.

BE 9 Thermoreflectance of Organic and Polymeric Metals. P. M. GRANT, P. MENGEL, E. M. ENGLER, G. CASTRO and G. B. STREET, IBM Research Laboratory, San Jose, Calif.--We have examined the thermoreflectance spectrum of $(SN)_x$ crystals and films and of (TTF)(TCNQ) and (TSeF)(TCNQ) crystals in energy ranges appropriate to their Drude properties and low-lying interband transitions as a function of temperature from 300°K to 15°K. In $(SN)_x$, we observe a red shift of the Drude edge which we associate with movement of the Fermi level due to volume effects. Perov and Fischer[1] have reported polarization effects in the thermoreflectance spectrum of (TTF)(TCNQ) connected with the Peierls-Fröhlich transition. We have made similar measurements on (TSeF)TCNQ and compare our results with theirs for (TTF)(TCNQ).

[1]P. I. Perov and J. E. Fischer, Phys. Rev. Letters 33, 521 (1974).

BE 10 Calculated Optical Properties of $(SN)_x$. I. B. ORTENBURGER, W. E. RUDGE and P. M. GRANT, IBM Research Laboratory, San Jose, Calif.--The tensorial dielectric constant $\varepsilon_2(\omega)$ and the tensorial photoemission yield $D(E,\omega)$ have been calculated for $(SN)_x$ using a pseudo-potential interpolation scheme based on a first principles OPW band structure. $D(E,\omega)$ and $\varepsilon_2(\omega)$ were computed by the Gilat-Raubenheimer zonal integration method. Our results will be compared to experimental photoemission and optical[1] measurements on randomly oriented $(SN)_x$ films.

[1]A. A. Bright and A. F. Garito, to be published.

BE 11 Molecular Cluster and Band Structure Calculations for $(SN)_x$. D. R. SALAHUB and R. P. MESSMER, General Electric.--Molecular cluster and band structure calculations for $(SN)_x$ show that (i) a single $(SN)_x$ chain should be a Peierls insulator, (ii) semi-metallic behavior is brought about by interchain coupling which moves the Fermi level from the Peierls gap to a place where it intersects two bands, (iii) the most important interactions occur in a 100 plane, and not as previously assumed in a $\bar{1}02$ plane. Important aspects of the electronic structure of intermediates involved in the polymerization and subliniation of $(SN)_x$ are also discussed.

BE 12 Band Structure, Density of States, and Fermi Surface Topology of the $(SN)_x$ Crystal.* W. Y. CHING, J. G. HARRISON, and CHUN C. LIN, U. of Wisconsin-

- We have derived the optical, photoemission and transport properties of $(SN)_x$ using Gilat-Raubenheimer techniques applied to a pseudopotential band structure and Fermi surface obtained by a fit to the the OPW results. Generally good agreement is obtained with measured film and single crystal reflectivities and with film UPS data. We predict the principal directions and anisotropies for hole-electron transport effects with respect to crystallographic axes.

- Brief review of theory with respect to tensorial nature of $\varepsilon_2(\omega)$ and $\mathcal{D}(E,\omega)$. Calculation of normal incidence reflectivities and averaging for randomly oriented crystalline films. Form and meaning of the plasma tensor. Rotation into $(\bar{1}02)$ plane.

- Calculation of Drude and interband contributions to $R_\parallel$ and $R_\perp$. Form assumed for the Drude contribution:

$$\varepsilon^D_{\mu\nu}(\omega) = \frac{-(\omega_p^2)_{\mu\nu}}{\omega(\omega + i/\tau_{\mu\nu})}$$

The $(\omega_p^2)_{\mu\nu}$ were calculated and the $\tau_{\mu\nu}$ taken from experiment under the following assumptions

$$\tau_{yy} = 1.8\ \text{eV}^{-1} \quad (\text{Grant, Cohen})$$
$$\tau_{xx} = \tau_{zz} = \tau_{xz} = 0.57\ \text{eV}^{-1} \quad (\text{Cohen})$$

Total dielectric tensor is then $\varepsilon_{\mu\nu}(\omega) = \varepsilon^D_{\mu\nu} + \varepsilon^B_{\mu\nu}$ from whence $R_\parallel$ and $R_\perp$ are calculated once $\varepsilon_{\mu\nu}$ is rotated into the $(\bar{1}02)$ plane.

- Comparison with film reflectivity from 0-14 eV (Cohen) We find the best agreement between theory and experiment to occur for $(R_\parallel b)\div 2$ rather than for $(R_\parallel + R_\perp)\div 2$ expected for unpolarized light incident on an oriented film. This may be due to the

fact that the light emerging from the monochromater was indeed partially polarized along the b-axis of the oriented film (This possibility will be checked out with Cohen).

Origin of the structure in ϵ_{2yy}^B and ϵ_{2xx}^B. The structure for these components falls into three broad categories insofar as they influence experimental results:

A. < 1 eV. Structure in this region arises primarily from transition between parallel bands near the Fermi level along $\Gamma \Delta Z$ near Z and halfway between Z and E. The latter have a strong influence on the properties of $R \perp b$.

B. 2-3 eV. Stronger effects in both theory and experiment are observed for $E \perp b$. The nearly parallel bands between ΓA and $Z E$ may be responsible for these transition.

C. 4-8 eV. For $E \parallel b$, these transition may arise from the parallel bands along DVB, whereas for $E \perp b$, parallel bands in the same energy range along ZE seem likely candidates.

Comparison with the single crystal data of Grant and colleagues. For $R \parallel b$, the agreement is deemed to be qualitatively excellent and quantitatively satisfactory. Especially pleasing is the closeness of the calculated and experimental plasma energies. For $R \perp b$, we see the effect of the strong ZE interband transition arising as the 0.7 eV peak in the reflectivity. This structure is readily seen because of the very strongly damped nature of the Drude absorption in this energy range.

— Anisotropy of the plasma tensor. Many of the transport, optical and superconducting properties of a metal may be related to the plasma tensor which is the Fermi surface integral of the group velocity, viz:

$$(\omega_p^2)_{\mu\nu} = 4\pi e^2 \int_{S_F} dS \; \frac{v_\mu v_\nu}{|v|} \; ; \quad v_\mu = \frac{1}{\hbar} \frac{\partial E}{\partial k_\mu}$$

For metals or semi-metals with complicated band structures like $(SN)_x$, the plasma tensor occupies the role played by n/m^* in the theory of simple structures. We find the principal axes of the combined hole-electron plasma tensor in $(SN)_x$ to be nearly contained ($\approx 12°$) within and orthogonal to the $(\bar{1}02)$ plane and to be in the ratios $1 : 0.13 : 0.09$ with respect to the directions $b : (\bar{1}02)_{||} : (\bar{1}02)_{\perp}$. Thus we see that $(SN)_x$ is indeed a three dimensional semi-metal with the physical satisfying result that the principal axes of the anisotropy lie close to directions in which the greatest interchain interaction is to be expected.

PHOTORESPONSE FUNCTIONS

OPTICAL:

$$\varepsilon_{2\mu\nu}(\omega) = \frac{e^2}{\pi m^2 \omega^3} \sum_{nn'} \int d^3k \; f_n (1 - f_{n'})$$

$$\times \; \langle n\vec{k} | p_\mu | n'\vec{k} \rangle \langle n'\vec{k} | p_\nu | n\vec{k} \rangle$$

$$\times \; \delta \left(E_{n'}(\vec{k}) - E_n(\vec{k}) - \hbar\omega \right)$$

$$\left(\omega_p^2 \right)_{\mu\nu} = 4\pi e^2 \int_{S_F} dS \; \frac{v_\mu v_\nu}{|v|} \quad ; \quad v_\mu = \frac{1}{\hbar} \frac{\partial E}{\partial k_\mu}$$

PHOTOEMISSION

$$D_{\mu\nu}(E,\omega) = \frac{e^2}{\pi m^2 \omega^2 \langle \varepsilon_2(\omega) \rangle} \sum_{nn'} \int d^3k \; f_n (1 - f_{n'})$$

$$\times \; \langle n\vec{k} | p_\mu | n'\vec{k} \rangle \langle n'\vec{k} | p_\nu | n\vec{k} \rangle$$

$$\times \; \delta \left(E_{n'}(\vec{k}) - E_n(\vec{k}) - \hbar\omega \right)$$

$$\times \; \delta \left(E_{n'}(\vec{k}) - E \right)$$

REFLECTIVITY OF MONOCLINIC $(SN)_x$

$$\epsilon(\omega) = \begin{pmatrix} \epsilon_{xx} & 0 & \epsilon_{xz} \\ 0 & \epsilon_{yy} & 0 \\ \epsilon_{xz} & 0 & \epsilon_{zz} \end{pmatrix}$$

$$\epsilon_{\mu\nu}(\omega) = \epsilon_{\mu\nu}^{D} + \epsilon_{\mu\nu}^{B}$$

where

$$\epsilon_{\mu\nu}^{D} = \frac{-(\omega_p^2)_{\mu\nu}}{\omega(\omega + i/\gamma_{\mu\nu})} = \frac{-\omega_p^2(\omega - i/\gamma)}{\omega(\omega^2 + 1/\gamma^2)} \underset{\epsilon_2}{\Longrightarrow} \frac{\omega_p^2 \gamma}{\omega(1 + \omega^2\gamma^2)}$$

and $\epsilon_{\mu\nu}^{B} =$ Interband Components from EPM

From Fresnel Determinant:

$$n_{\parallel}^2 = \epsilon_{yy}$$

$$n_{\perp}^2 = \epsilon_{xx} - \epsilon_{xz}^2/\epsilon_{zz}$$

From Normal Incidence Equations:

$$R_{\parallel} = \left| \frac{n_{\parallel} - 1}{n_{\parallel} + 1} \right|^2 \qquad ; \qquad R_{\perp} = \left| \frac{n_{\perp} - 1}{n_{\perp} + 1} \right|^2$$
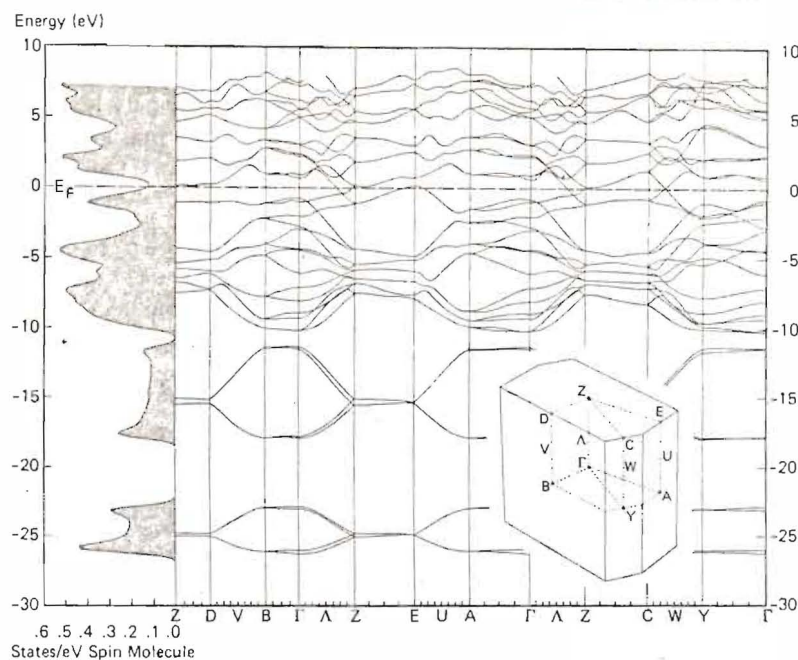
FIG. 1. OPW energy bands for $(SN)_x$, Lyon structure. The density-of-states curve on the left was obtained by placing a Gaussian function with half-width equal to 0.25 eV on each energy level and summing over the 128 points sampled in the Brillouin zone. The zone itself is shown in the inset. The energy scale was chosen to put the Fermi level at zero.

to a total of 550 OPW's, was employed. The crystal potential was created by superposing sulfur and nitrogen atomic potentials, which were in turn computed using the Kohn-Sham statistical exchange model.[20] Use of Slater exchange[27] broadened the bands somewhat and lowered the lowest core level by about 2 eV. Here we report the Kohn-Sham results exclusively. The calculation was nonrelativistic and non-self-consistent.[22] Convergence was tested by doubling the basis set
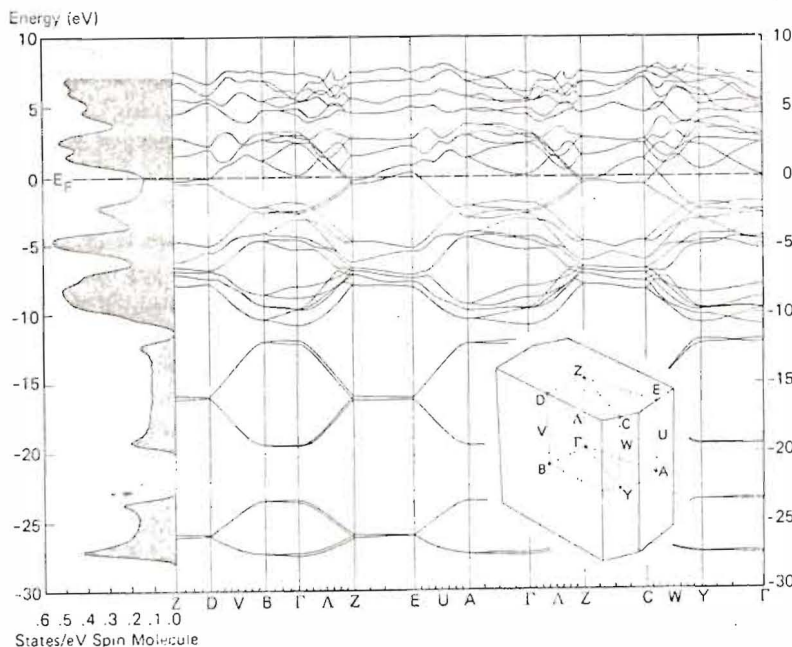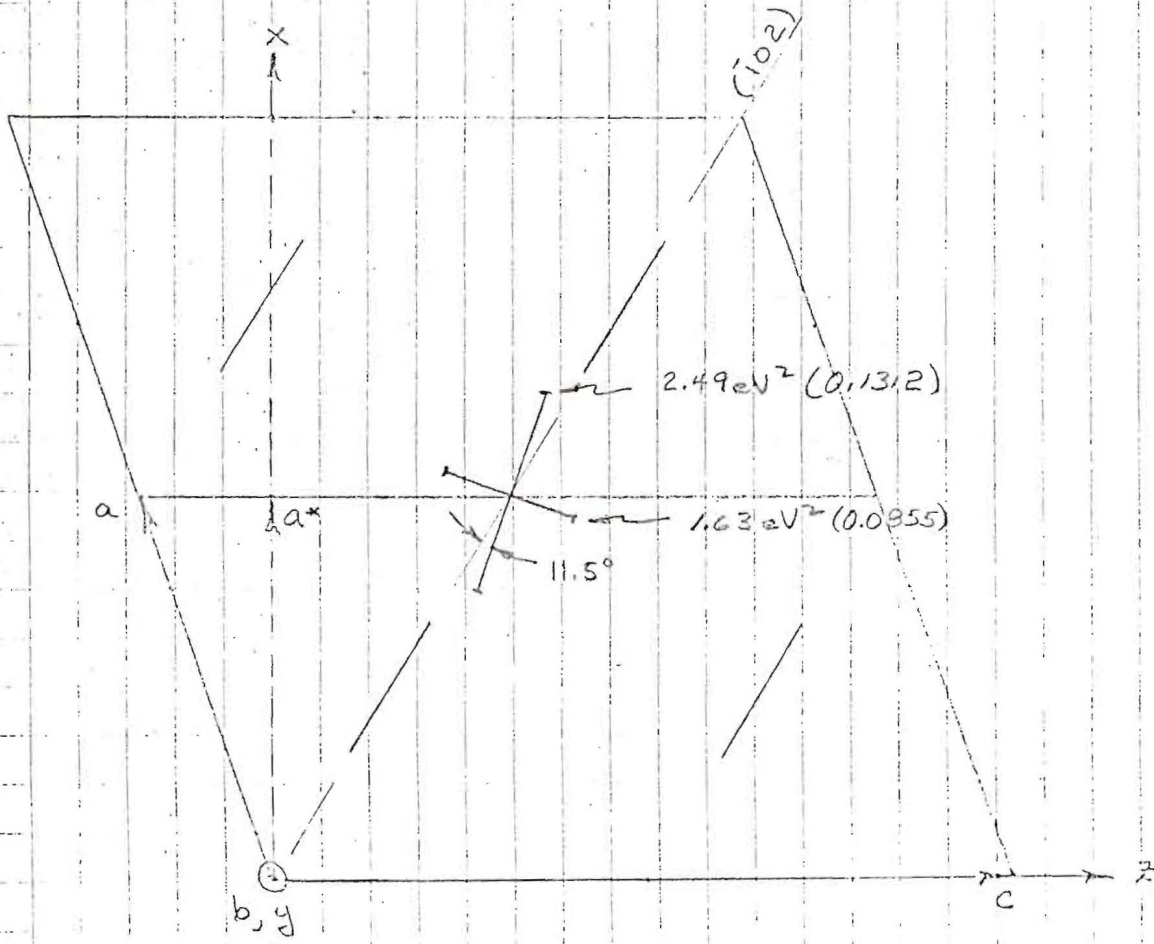

FIG. 2. OPW energy bands for $(SN)_x$, Penn structure. The density of states was obtained as for Fig. 1.

b-axis Projection of (SN)x Unit Cell

Cell Parameters:

$a = 4.153$ Å
$b = 4.439$
$c = 7.637$

$a^* = 3.910$
$\beta = 109.7°$

2.49 eV^2 (0,13,2)

1.63 eV^2 (0.0955)

11.5°

Scale for b-axis ω_b^2

19.01 eV^2 (1)

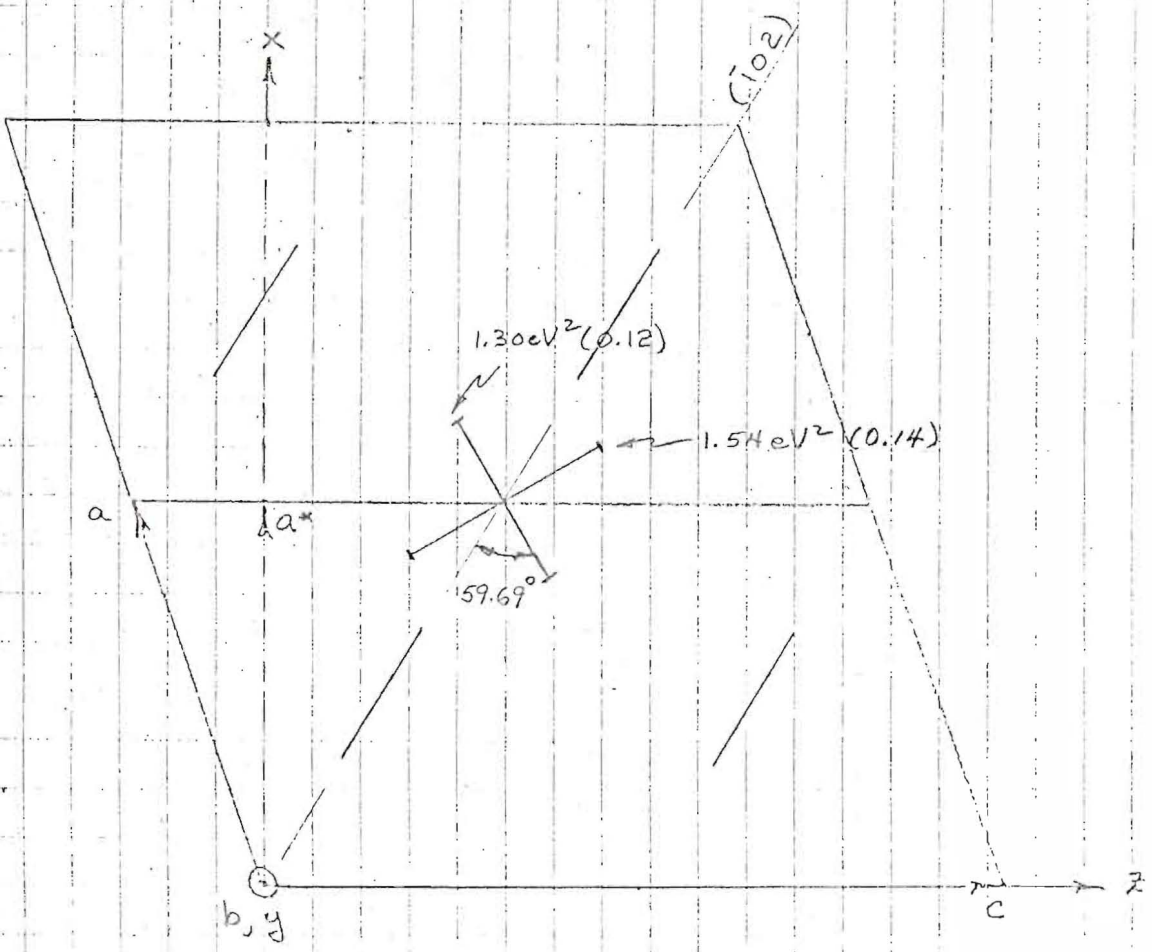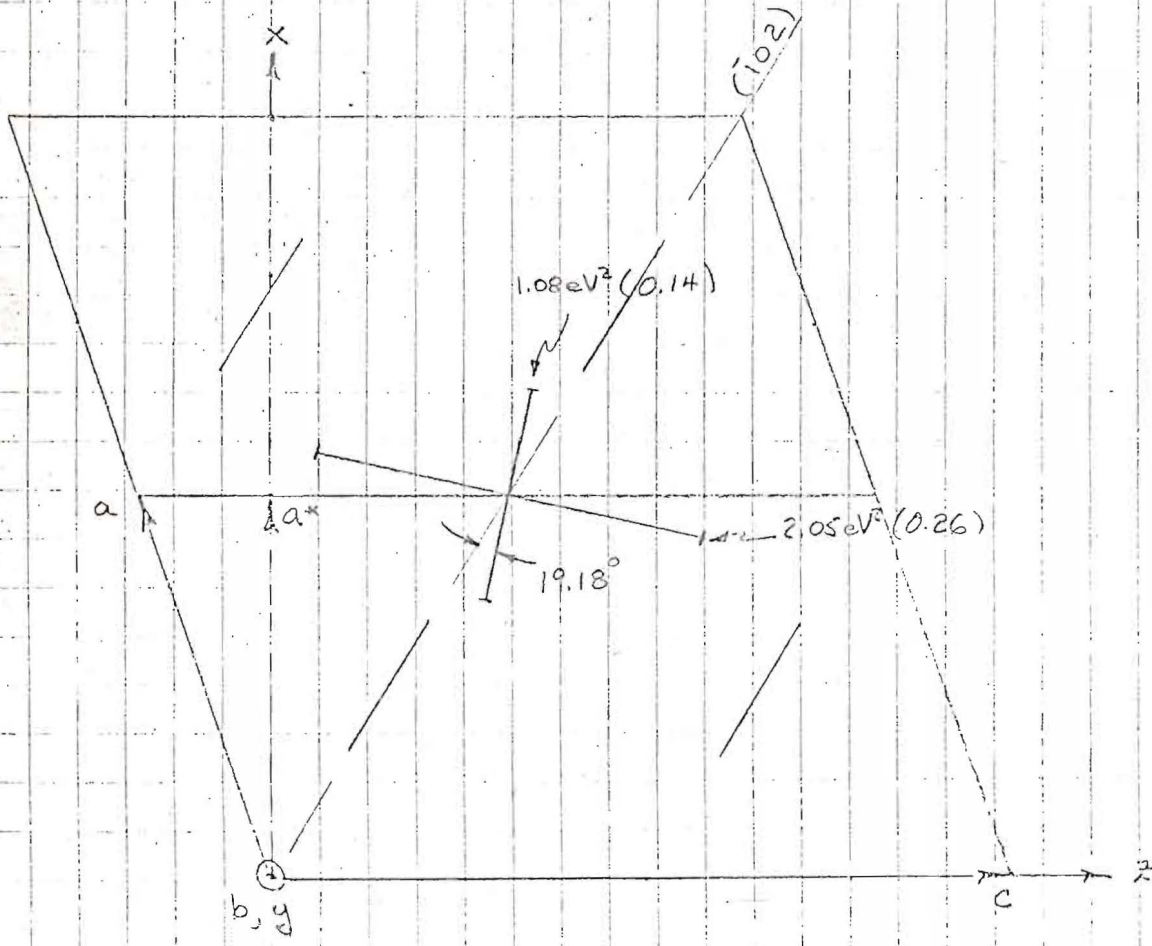PLASMA TENSOR PRINCIPAL AXES FOR COMBINED HOLES AND ELECTROIDS

b-axis Projection of (SN)ₓ Unit Cell

Cell Parameters: $a = 4.153$ Å $a^* = 3.910$

                   $b = 4.439$ $\beta = 109.7°$

                   $c = 7.637$

Scale for b-axis ω_p^2

11.142 eV² (1)

PLASMA TENSOR PRINCIPAL AXES

ALL HOLES

b-axis Projection of (SN)x Unit Cell

Cell Parameters: $a = 4.153$ Å $a^* = 3.910$
                    $b = 4.489$ $\beta = 109.7°$
                    $c = 7.637$

1.08 eV² (0.14)

2.05 eV² (0.26)

19.18°

Scale for b-axis ω_p^2

7.37 eV² (1)

PLASMA TENSOR PRINCIPAL AXES

ALL ELECTRONS